

the bandwidth is small compared to f_c , it can be calculated with eqn. 2:

$$\Delta f = \frac{f_c}{\pi} \cos^{-1} \frac{1 + b^2 - 2a^2}{2b} \quad (6)$$

The quality factor Q is given by

$$Q = \frac{f_c}{\Delta f} = \frac{\pi}{\cos^{-1} \frac{1 + b^2 - 2a^2}{2b}} \quad (7)$$

Note that the centre frequency is equal to f_c , the bandwidth is proportional to f_c , and Q , which can reach very high values, is independent of f_c . These are all qualities that make N -path filters interesting for many applications.

In contrast to known SC N -path filters with lowpass cells, the presented FIR N -path filter does not need a bandpass prefilter to filter out the bandpass range at f_c . All that is necessary is a lowpass prefilter that can also be built with grounded capacitors.

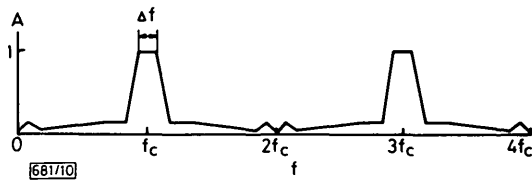


Fig. 10

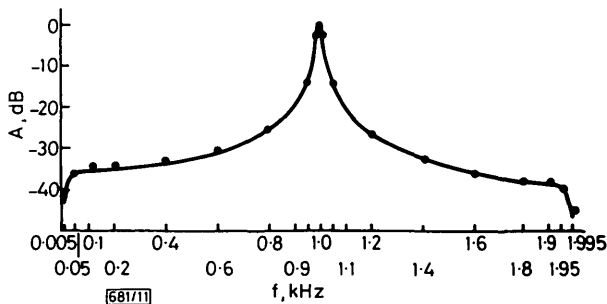


Fig. 11

— predicted
 measured

The SC FIR 4-path filter of Fig. 9 has been breadboarded using discrete IC components ($C_1/C_2 = 1/14.63$, $f_c = 1$ kHz). The measurements confirmed the theory presented as shown in Fig. 11. The number of clock phases can be halved by introducing more switched capacitors. The tradeoff between clock phases and the number of switched capacitors depends on the application in question.

D. von GRÜNIGEN
 U. W. BRÜGGER
 G. S. MOSCHYTZ

19th August 1981

Institute of Telecommunications
 Swiss Federal Institute of Technology
 CH-8092 Zurich, Switzerland

W. VOLLENWEIDER
 Autophon AG
 Solothurn, Switzerland

References

- 1 ALLSTOT, D. J., and TAN, K. S.: 'A switched capacitor N -path filter'. Proceedings of IEEE ISCAS, Houston, Apr. 1980, pp. 313-316
- 2 LEE, M. S., and CHANG CH.: 'Exact synthesis of N -path switched-capacitor filters'. Proceedings of IEEE ISCAS, Chicago, Apr. 1981, pp. 166-169
- 3 GHADERI, M. B., TEMES, G. C., and NOSSEK, J. A.: 'Switched-capacitor pseudo- N -path filters', *ibid.*, pp. 519-522
- 4 DESSOULAVY, R., KNOB, A., KRUMMENACHER, F., and VITTOZ, E. A.: 'A synchronous switched capacitor filter', *IEEE J. Solid-State Circuits*, 1980, SC-15
- 5 FRANKS, L. E., and SANDBERG, I. W.: 'An alternative approach to the realization of network functions: The N -path filter', *Bell Syst. Tech. J.*, 1960, pp. 1321-1350

0013-5194/81/210788-03\$1.50/0

GROOVE GaInAsP LASER ON SEMI-INSULATING InP

Indexing terms: Lasers, Semiconductor lasers, Semi-insulating compounds

A new GaInAsP/InP injection laser was fabricated on semi-insulating substrates. The structure utilises a single LPE growth process on a grooved substrate to form an index guided device. Current confinement was obtained by the semi-insulating InP surrounding the GaInAsP active layer. Threshold current as low as 28 mA with 250 μm cavity length was obtained. The light/current characteristic was linear up to five times I_{th} . A single longitudinal mode at 1.20 μm up to 1.3 I_{th} was observed.

Introduction: The quaternary GaInAsP/InP buried heterostructure (BH) laser has gained considerable interest in recent years as a promising light source for fibre optical communication in the range of 1.0-1.7 μm . Integration of several optoelectronic devices such as detectors and bipolar or field effect transistors with laser diodes would bring a significant improvement in simplicity, reliability and high frequency performance of future systems. Electrical isolation of individual components can be achieved by using a semi-insulating (SI) substrate, as was recently demonstrated with several GaAs devices.¹⁻³ Thus there is a strong motivation for developing simple, low threshold lasers on SI InP substrates. A BH injection laser on SI InP was recently reported.⁴

In BH lasers, the electrical current confinement is accomplished by growing layers of reverse biased junctions on both sides of the active junction. The leakage current in BH lasers is determined by the exact positioning of the reverse biased junctions.

The present work describes a new groove laser diode, which is illustrated in Fig. 1, fabricated on SI substrate utilising the SI material to provide electrical current confinement. This forces the injection current to flow through the active region. The leakage through regions of surrounding SI InP, which have very high specific resistivity, is reduced to negligible proportions.

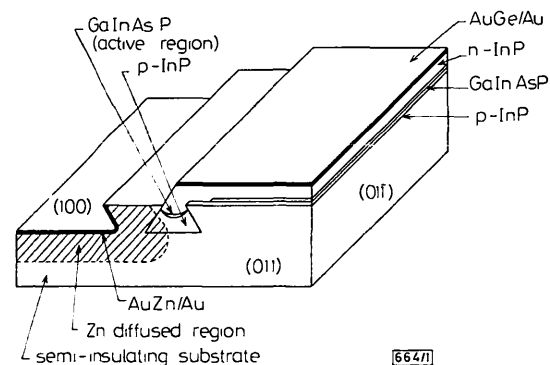


Fig. 1 Schematic cross-section of groove laser

The groove laser is relatively simple to fabricate since it requires only a single epitaxial growth step. There is no regrowth and thus no need for the alignment of the reverse biased junctions. Still, it provides the necessary optical and electrical confinement for low threshold operation. Further advantages of the groove laser are the small current path distance and minimal stray capacitance associated with this structure.

Structure and fabrication: The structure of the laser diode is schematically shown in Fig. 1. An SEM view of the cleaved cross-section is shown in Fig. 2.

The structure was realised by etching dovetail shaped grooves^{5,6} in the SI InP substrate through CVD Si_3N_4 stripe openings. The stripes were made in the [011] direction and were 3.5 μm wide. The etchant used was 10% solution of iodic acid in water. This etchant produced sharp grooves with well defined straight lined cross-sections. The etching rate was slow

and reproducible ($\sim 1200 \text{ \AA}/\text{min}$ at 22°C) and smooth surfaces were obtained.

The shape of the etched groove is direction dependent. For stripes in the $[011]$ direction a dovetail shape is obtained, while a V-groove is formed in the $[0\bar{1}\bar{1}]$ direction. A cross-section of the etched grooves in both direction is shown in Fig. 3. It had been noticed⁵ that for GaInAsP/InP system the growth profile on grooved channels strongly depends on the initial etched profile. For the V-groove shape the growth in the groove is usually isolated from the rest of the wafer because of slow growth rate on the (111) and $(1\bar{1}\bar{1})$ side walls of the V-groove. The shape of the growth in the $[0\bar{1}\bar{1}]$ channels is therefore less reproducible than in the $[011]$ direction. Channels in the $[011]$ direction were preferred for the present structure.

After the etching of the groove, the Si_3N_4 was selectively removed from one side of the groove. The remaining Si_3N_4 on the other side of the groove acted as a mask on which no growth occurred during epitaxy.⁷

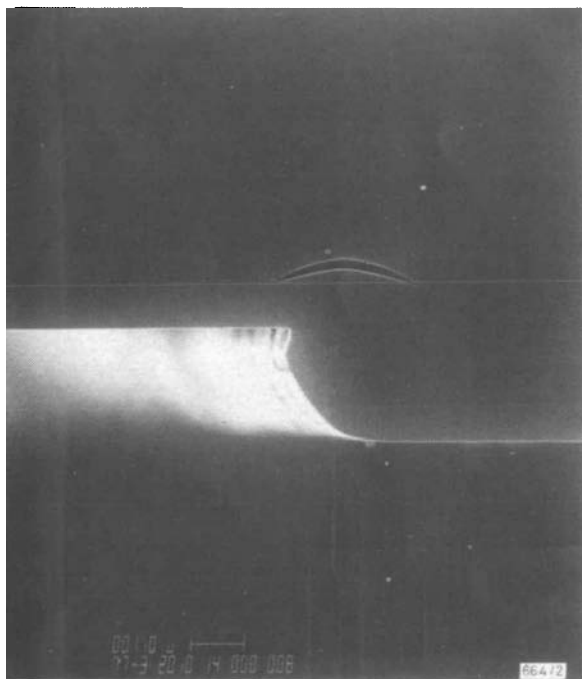


Fig. 2 SEM view of layers after LPE growth

Three LPE layers were subsequently grown on the wafer, a P-type InP layer ($4 \times 10^{17} \text{ cm}^{-3}$ Zn doped) a GaInAsP quaternary layer (undoped) and an N-type InP ($2 \times 10^{18} \text{ cm}^{-3}$ Sn doped). The first layer was grown from a 5°C super-cooled solution while the active layer and the third layer were grown from two-phase solutions. The quaternary growth temperature was 635°C . The cooling rate for the first two layers was $0.1\text{--}0.2^\circ\text{C}/\text{min}$. The cooling rate was increased to $1^\circ\text{C}/\text{min}$ for the last layer. The growth of the first layer was quite critical. It determined the width of the active layer and its height above the bottom of the groove. By adjusting the position of the active layer, we can control the optical confinement of the resulting waveguide.

Following the LPE a new Si_3N_4 layer was deposited and windows for diffusion were opened. Through these windows the InP was etched with 0.5% solution of Br_2 in methanol. Subsequently a Zn diffusion was performed which penetrated the LPE grown P-type InP (see Fig. 1). After the diffusion AuZn/Au was evaporated and photolithographically defined followed by annealing at 420°C . Then the AuGe/Au contact was evaporated and defined using the standard lift-off technique, and annealed at 300°C . The two resulting contacts have broad areas and are reliable and easy to connect to output terminals.

Performance: The light/current characteristic of the laser is shown in Fig. 4. A typical threshold current was 35 mA and the lowest pulsed threshold achieved was 28 mA . The characteristics are linear up to five times the threshold current. For CW operation, the laser was mounted on a gold plated copper

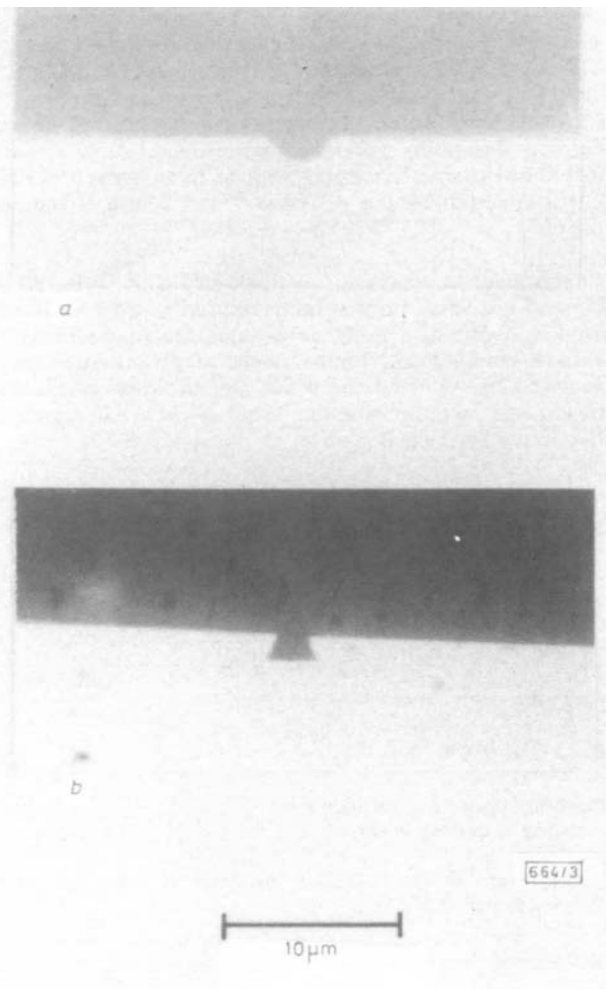


Fig. 3 Cross-sectional views of etched grooves
a $[011]$ direction
b $[0\bar{1}\bar{1}]$ direction

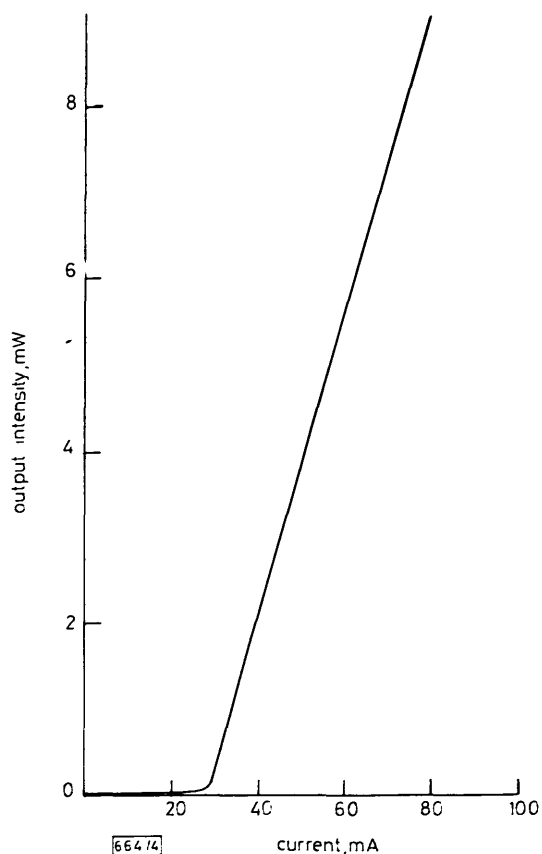


Fig. 4 Light/current characteristics of a laser at pulsed operation, $I_{th} = 28 \text{ mA}$

block, substrate side down. The threshold current for CW operation was typically 20% higher than for pulsed operation. The external differential quantum efficiency for both facets was 40%. Single longitudinal mode was observed at up to 1.3 threshold current. Multimode operation was obtained at higher currents. The lasing wavelength was around 1.2 μm . The above mentioned characteristics correspond to an active layer of 3.0 μm width and 0.4 μm thickness at the centre of the active region.

Conclusions: In conclusion, a single-step LPE GaInAsP laser on semi-insulating InP has been reported. Low threshold operation was obtained using novel semi-insulating structure for current confinement. Improvement in performance may be achieved by reducing the width and thickness of the active region and by optimising the height of the active region relative to the pre-etched groove.

Acknowledgments: The authors wish to thank Dr. N. Bar-Chaim of California Institute of Technology for helpful discussions and P. Koen of California Institute of Technology for taking the scanning electron microscope (SEM) pictures. This work is supported by the US Office of Naval Research and by the National Science Foundation.

K. L. YU
U. KOREN
T. R. CHEN*
P. C. CHEN
A. YARIV

17th August 1981

California Institute of Technology
Pasadena, California 91125, USA

* Permanent address: Chengdu Institute of Radio Engineering, People's Republic of China

References

- 1 URY, I., MARGALIT, S., YUST, M., and YARIV, A.: 'Monolithic integration of an injection laser and a metal semiconductor field effect transistor', *Appl. Phys. Lett.*, 1979, **34**, pp. 430-431
- 2 YUST, M., BAR-CHAIM, N., IZADPANAH, S. H., MARGALIT, S., URY, I., WILT, D., and YARIV, A.: 'A monolithically integrated optical repeater', *ibid.*, 1979, **35**, pp. 795-797
- 3 WILT, D., BAR-CHAIM, N., MARGALIT, S., URY, I., YUST, M., and YARIV, A.: 'Low threshold Be implanted (GaAl)As laser on semi-insulating substrate', *IEEE J. Quantum. Electron.*, 1980, **QE-18**, pp. 390-391
- 4 MATSUOKA, T., TAKAHEI, K., NOGUCHI, Y., and NAGAI, H.: '1.5 μm region InP/GaInAsP buried heterostructure lasers on semi-insulating substrates', *Electron. Lett.*, 1981, **17**, pp. 12-14
- 5 MUROTANI, T., OOMURA, E., HIGUCHI, H., NAMIZAKI, H., SUSAKI, W.: 'InGaAsP/InP buried crescent laser emitting at 1.3 μm with very low threshold current', *ibid.*, 1980, **16**, pp. 566-568
- 6 OLSEN, G. H., and ZAMEROWSKI, T. J.: 'Vapour phase growth of (InGa)(AsP) quaternary alloys', *IEEE J. Quantum. Electron.*, 1981, **QE-17**, pp. 128-137
- 7 CHEN, P. C., YU, K. L., MARGALIT, S., and YARIV, A.: 'Embedded epitaxial growth of low threshold GaInAsP/InP injection lasers', *Appl. Phys. Lett.*, 1981, **38**, p. 301

0013-5194/81/210790-03\$1.50/0

CAUER CONTINUED FRACTION METHODS FOR MODEL REDUCTION

Indexing terms: Modelling, Linear systems, Model reduction, Cauer continued fractions

This letter surveys the recently published methods for deriving stable reduced-order models and justifies how sophisticated techniques had to be evolved to meet different problems which arise in the reduction of high-order systems.

Introduction: In Reference 12, Shamash's criticisms of the recently proposed methods include a sharp critique of our position in this problem. He has apparently drawn his

conclusions from some examples of low-order systems where Gustafson's truncation method¹ would, indeed, suffice.

Model using modified Cauer form with Routh approximation: In this letter we trace the development of sophisticated techniques to meet different problems which arise in model reduction. Specifically, we confine ourselves to continued fraction methods which are a special case of Padé approximation. It is well known that these methods may produce unstable reduced-order models, although the original system may be stable.

Chen and Shieh² pioneered the application of the continued fraction technique to model-reduction problems. To achieve a better approximation of the initial transient response of the system, Chuang³ modified the continued fraction expansion by combining expansion about $s = 0$ and $s = \infty$ alternately. A computerised algorithm to perform the expansion and inversion of this Cauer form, called the modified Cauer form (MCF), has been reported earlier.⁷ It was found that this algorithm would not guarantee the stability of the reduced models.

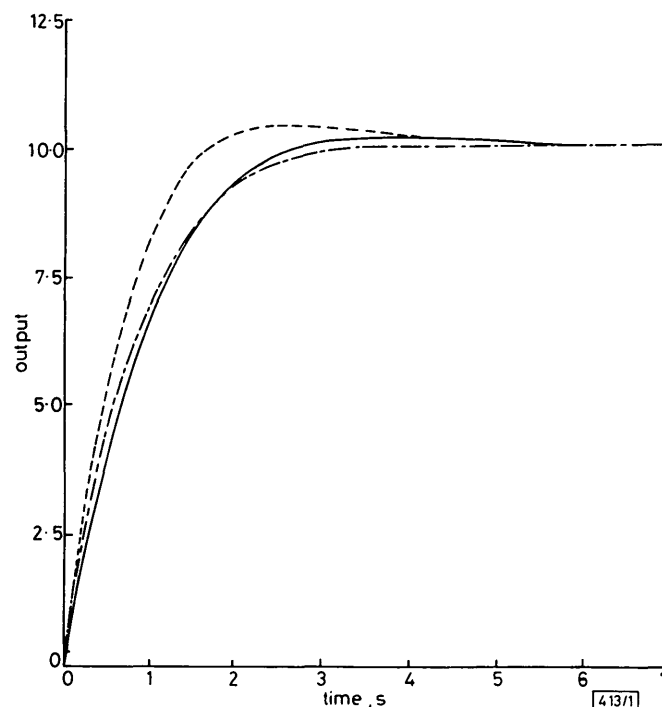


Fig. 1 Step responses of original 4th-order system and reduced-order models obtained by Routh approximation and matching MCF quotients

— original system
- · - · 3rd-order model
- - - 2nd-order model

So we have combined⁹ Routh approximation with matching a set of initial quotients in the MCF of the original systems, inducting the principle given by Power.⁶ This gives a better approximation than that derived by Shamash's method,⁵ which fits only the initial time moments of the system. Applying this technique to the transfer function^{5,11}

$$G(s) = \frac{1200 + 900s + 248s^2 + 14s^3}{12 + 180s + 102s^2 + 18s^3 + s^4}$$

we get the different approximants as

$$R_3(s) = \frac{75 + (225/4)s + 14s^2}{(15/2) + (45/4)s + (151/21)s^2 + s^3}$$

and

$$R_2(s) = \frac{40 + 42s}{4 + 6s + s^2}$$

The step response is plotted in Fig. 1, which shows that the 3rd-order model is quite close to the given system.